Propagation of phase-locked truncated Gaussian beam array in turbulent atmosphere*

Zhou Pu(周 朴), Liu Ze-Jin(刘泽金)†, Xu Xiao-Jun(许晓军), and Chu Xiu-Xiang(储修祥)

College of Optoelectric Science and Engineering, National University of Defense Technology, Changsha 410073*, China*

(Received 30 March 2009; revised manuscript received 23 July 2009)

Truncation manipulation is a simple but effective way to improve the intensity distribution properties of the phase-locked Gaussian beam array at the receiving plane. In this paper, the analytical expression for the propagation of the phase-locked truncated Gaussian beam array in a turbulent atmosphere is obtained based on the extended Huygens–Fresnel principle. Power in the diffraction-limited bucket is introduced as the beam quality factor to evaluate the influence of different truncation parameters. The dependence of optimal truncation ratio on the number of beamlets, the intensity of turbulence, propagation distance and laser wavelength is calculated and discussed. It is revealed that the optimal truncation ratio is larger for the laser array that contains more lasers, and the optimal truncation ratio will shift to a larger value with an increase in propagation distance and decrease in intensity of atmosphere turbulence. The optimal truncation ratio is independent of laser wavelength.

Keywords: laser array, phase locking, truncation, propagation, turbulence

PACC: 4225B, 4225K, 9265R

1. Introduction

The phase-locked beam array has been under intense research recently due to the potential ability in solving power limitation in a single laser caused by medium inhomogeneity, heat management as well as maintaining good beam quality.[1−8] The propagation properties of the phase-locked beam array have also been studied in detail.[9−15] To date, the highest power demonstrations for phase locking involved tiling an array of beamlets in a close-packed configuration to form a composite output beam.[2,3,5] This unavoidably leads to a loss of beam quality as compared to a fully filled, uniform (i.e., flat-top) near field.[1,6−8] In particular, for phase locking Gaussian-mode beamlets emitted from fibre lasers or amplifiers, the beam quality suffers degradation due to the tiling low fill factor of Gaussian beamlets. Four fibre laser beamlets distributed in a 2×2 laser array have successfully formed a 470-W phase-locked output beam,[3] only 63% of the whole laser power is contained within the far-field central main-lobe. Several possible methods have been developed to increase the power channeled into the central far-field lobe. One solution is to combine the beamlets on top of one another using diffractive optical elements.[6] One can also substantially increase encircled far-field central-lobe energy by shaping the near field energy distribution of radiation from each fibre to flat-topped beams.[5,16] More recently, waveguide beam combiners and phase elements have been developed to convert light from a sparse array into a single-lobed far-field one with a theoretical efficiency approaching 100%.[17,18] However, these approaches involved complicated optical design or additional optical elements. One simple approach is truncating the outgoing Gaussian beam to obtain a more uniform intensity distribution at the expense of energy loss.[19] Increasing the beam spot size to better fill the aperture will thus decrease the far-field energy spreading into side-lobes, but it will also cause increasing energy loss as the Gaussian beam is truncated by the finite-diameter aperture. Thus a tradeoff should be performed between the energy loss due to beam truncating and improvement in fill factor by evaluating the far-field patterns. The optimal truncation ratio for each beamlet in the phased array has been studied when propagating in free-space;[19,20] in addition, the propagation properties of various kinds of phase-locked beam array have been studied in detail,[9−15] yet to the best of our knowledge the propagation of phase-locked truncated Gaussian beam arrays in turbulent atmosphere has not been investigated. In the present paper, we will focus on the propagation of a

*Project supported by the Innovation Foundation for Postgraduate of Hunan Province.

†Corresponding author. E-mail: zejinliu@vip.sina.com

© 2010 Chinese Physical Society and IOP Publishing Ltd

phase-locked truncated Gaussian beam array in turbulent atmosphere. The effect of the truncation of beamlets on the beam quality in the target-plane is evaluated by the power-in-the-bucket (PIB) metric. The dependence of the optimal truncation ratio on the number of beamlets, the intensity of turbulence, propagation distance and laser wavelength will be calculated and discussed. Through this work we hope to offer some reference for designing the phase-locked beam array system in practical engineering fields such as energy delivering and free-space communication.

2. Analysis of theory

2.1. Analytical expression of the average intensity at z-plane

We assume that the phase-locked beam array located at the source plane ($z = 0$) is arranged in the form of a hexagonal array of densely packed circular sub-apertures, as shown in Fig. 1. The system aperture diameter D is defined by a circle of smallest diameter that contains all the sub-apertures.[19] The laser beams propagate along the z axis in the Cartesian coordinate system. The optical field of the phase-locked beam array at the source plane can be expressed as

$$E(x, y, z = 0) = \sum_{m=1}^{M} E_m(x, y, z = 0)\, t_m(x, y, 0), \quad (1)$$

where $E_m(x, y)$ denotes the m-th Gaussian beam with the beam width ω_0, located at the positions (a_m, b_m), which can be expressed as

$$E_m(x, y, 0) = \exp\left[-\frac{(x - a_m)^2 + (y - b_m)^2}{w_0^2}\right], \quad (2)$$

and $t_m(x, y, 0)$ is the window function of hard-aperture that truncates the Gaussian beam and can be expressed as

$$t_m(x, y, 0) = \sum_{j=1}^{N} B_j \exp\left\{-\frac{C_j}{a^2}\left[(x - a_m)^2 + (y - b_m)^2\right]\right\}. \quad (3)$$

In Eq. (3) the complex constants B_j and C_j are the expansion and Gaussian coefficients, respectively, which can be obtained by optimization computation directly.[21,22] And a denotes the sub-aperture radius.

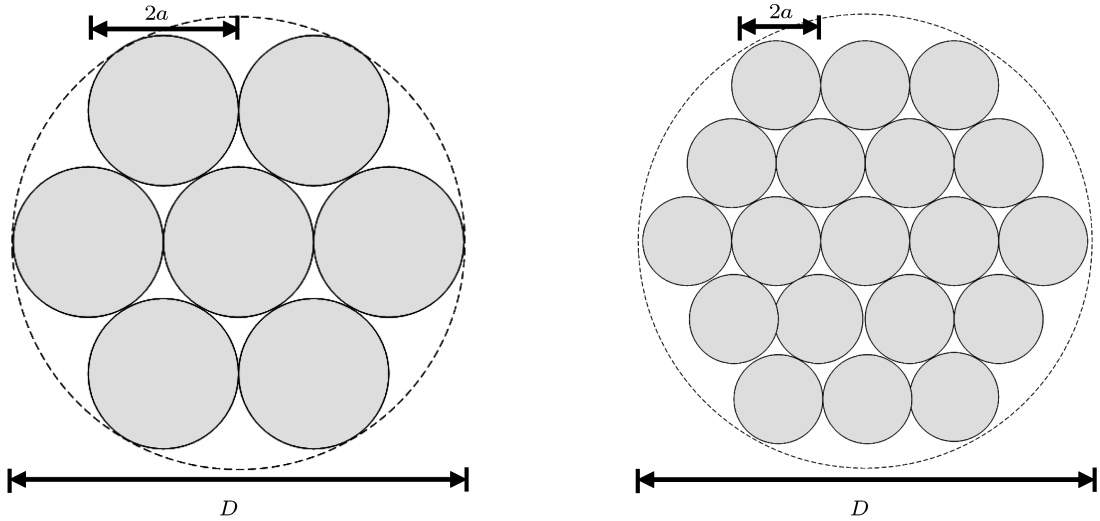


Fig. 1. Schematic diagram of the laser beam array.

By using the extended Huygens–Fresnel principle, the average intensity of the truncated phase-locked beam array at the z-plane after propagating in the turbulent atmosphere can be expressed as [9−15,23,24]

$$\begin{aligned}\langle I(p, q, z)\rangle = \frac{k^2}{(2\pi z)^2} \int_{-\infty}^{\infty}\int_{-\infty}^{\infty}\int_{-\infty}^{\infty}\int_{-\infty}^{\infty} \langle E(x, y, 0)\, E^*(\xi, \eta, 0)\rangle \\ \times \exp\left\{\frac{\mathrm{i}\,k}{2z}\left[(p - x)^2 + (q - y)^2 - (p - \xi)^2 - (q - \eta)^2\right]\right\} \\ \times \langle \exp[\psi(x, y, p, q) + \psi^*(x, y, p, q)]\rangle\, \mathrm{d}x\mathrm{d}y\mathrm{d}\xi\mathrm{d}\eta, \end{aligned} \quad (4)$$

where $k = 2\pi/\lambda$ (λ is the laser wavelength), (p, q) denotes the transverse coordinate at the target plane, $\psi(x, y, p, q)$ denotes the random part of the complex phase of a spherical wave that propagates from the source point to the receiver point; the angle bracket indicates the ensemble average over the medium statistics covering the log-amplitude and phase fluctuations due to the turbulent atmosphere. In this paper, Kolmogorov spectrum and a quadratic approximation of the 5/3 power law for Rytov's phase structure function is employed. The last term in the integrand of Eq. (4) can be written as

$$\langle \exp[\psi(x, y, p, q) + \psi^*(\xi, \eta, p, q)] \rangle = \exp\left\{ -\frac{1}{\rho_0^2} \left[(x-\xi)^2 + (y-\eta)^2 \right] \right\}. \tag{5}$$

Here $\rho_0 = \left(0.545 C_n^2 k^2 z\right)^{-3/5}$ is the coherence length of a spherical wave propagating in turbulent atmosphere with C_n^2 being the structure constant.

By inserting Eqs. (1)–(3) and (5) into Eq. (4), we can express the average intensity of the truncated phase-locked laser beam array at the z-plane in the following form

$$\langle I(p, q, z) \rangle = \frac{k^2}{(2\pi z)^2} \sum_{m=1}^{M} \sum_{j=1}^{N} \sum_{n=1}^{M} \sum_{l=1}^{N} \Gamma_{mjnl}(p, q, z), \tag{6}$$

where

$$\begin{aligned} \Gamma_{mjnl}(p, q, z) = {} & \frac{k^2}{(2\pi z)^2} B_j B_l \\ & \times \int_{-\infty}^{\infty} \int_{-\infty}^{\infty} \int_{-\infty}^{\infty} \int_{-\infty}^{\infty} \exp\left\{ -\frac{[(x-a_m)^2 + (y-b_m)^2 + (\xi-a_n)^2 + (\eta-b_n)]}{w_0^2} \right. \\ & \left. - \frac{C_j[(x-a_m)^2 + (y-b_m)^2] + C_l[(\xi-a_n)^2 + (\eta-b_n)^2]}{a^2} \right\} \\ & \times \exp\left\{ \frac{\mathrm{i}k}{2z} [(p-x)^2 + (q-y)^2 - (p-\xi)^2 - (q-\eta)^2] \right\} \\ & \times \exp\left\{ -\frac{1}{\rho_0^2} [(x-\xi)^2 + (y-\eta)^2] \right\} \mathrm{d}x \mathrm{d}y \mathrm{d}\xi \mathrm{d}\eta. \end{aligned} \tag{7}$$

By using the integral formula Eq. (3.323.2) of Ref. [25] and perform the related integral, we can obtain

$$\Gamma_{mjnl}(p, q, z) = \frac{k^2 \pi}{(2z)^2} B_j B_l \exp\left(-\frac{a_m^2 + b_m^2}{w_m^2} - \frac{a_n^2 + b_n^2}{w_n^2} \right) \frac{1}{A_1 D_1} \exp\left(\frac{B_{1x}^2 + B_{1y}^2}{4A_1} + \frac{D_{2x}^2 + D_{2y}^2}{4D_1} \right), \tag{8}$$

where

$$\begin{aligned} & \frac{1}{w_m^2} = \frac{C_m}{a^2} + \frac{1}{w_0^2}, \quad \frac{1}{w_n^2} = \frac{C_n}{a^2} + \frac{1}{w_0^2}, \quad A_1 = \frac{1}{w_m^2} - \frac{\mathrm{i}k}{2z} + \frac{1}{\rho_0^2}, \quad A_2 = \frac{1}{w_n^2} + \frac{\mathrm{i}k}{2z} + \frac{1}{\rho_0^2}, \quad G = -\frac{2}{\rho_0^2}, \\ & B_{1x} = \frac{2a_m}{w_m^2} - \frac{\mathrm{i}kp}{z}, \quad B_{1y} = -\frac{2b_m}{w_m^2} - \frac{\mathrm{i}kq}{z}, \quad B_{2x} = -\frac{2a_n}{w_n^2} + \frac{\mathrm{i}kp}{z}, \quad B_{2y} = -\frac{2a_n}{w_n^2} - \frac{\mathrm{i}kq}{z}, \\ & D_1 = A_2 - \frac{G^2}{4A_1}, \quad D_{2x} = B_{2x} - \frac{B_{1x}G}{2A_1}, \quad D_{2y} = B_{2y} - \frac{B_{1y}G}{2A_1}. \end{aligned}$$

Equations (6) and (8) are the main analytical result of the present paper, which presents a convenient and effective way for studying the propagation properties of the truncated phase-locked Gaussian beam array in the turbulent atmosphere. The propagation properties of the phase-locked truncated Gaussian beam array in free space can be easily obtained by setting $\rho_0 = \infty$ in Eq. (8).

2.2. Evaluation for beam quality

In application fields such as beam energy delivering, the beam quality can be characterized by using the power-in-the-bucket (PIB) target-plane J_{PIB},[19,26] which is defined as the laser optical output power in a specified far-field bucket divided by

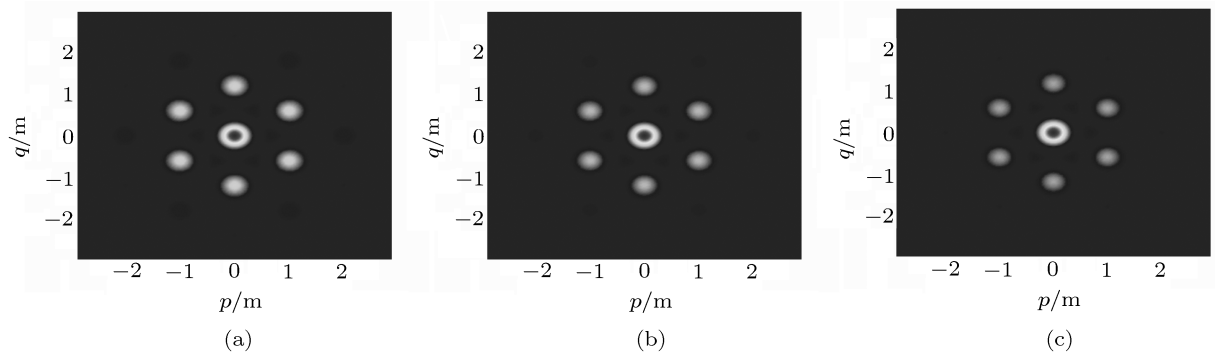
the total optical output power radiating from the effective near-field exit aperture of the laser beam array. The far field bucket radius r_T is usually defined as the diffraction limited radius $r_T^0 = 1.22\lambda z/D$,[19,25] where D is the effective exit aperture of the beam array. If we define the truncation ratio as $f = w_0/a$, $J_{\rm PIB}$ can be calculated by the following expression

$$J_{\rm PIB} = \int_{S_r} \langle I(p,q,z)\rangle \mathrm{d}^2\boldsymbol{r} \times \gamma(f) \Big/ \int_{-\infty}^{\infty} \langle I(p,q,z)\rangle \, \mathrm{d}^2\boldsymbol{r}, \tag{9}$$

where $S_r = \pi r_T^2$ is the area of the specified bucket, and $\gamma(f) = 1 - \exp\left(-2/f^2\right)$ is the ratio of outgoing beamlet power to the power of the Gaussian beam before truncation.[19] $\gamma(f)$ can be used to characterize the power loss due to the truncation manipulation. The optimization of design of the phase-locked beam array system should consider a tradeoff between fill factor improvement and power loss due to the truncation manipulation, that is, maximizing the value of $J_{\rm PIB}$.

3. Numerical calculation and analysis

In this section, we study the propagation properties of the truncated phase-locked laser beam array in turbulent atmosphere and the influence of related parameters. To study the propagation properties of the truncated phase-locked laser beam array, we calculate the intensity profile on the receiving plane for a hexagonal-distributed 7-laser array in turbulent atmosphere with different structure constants and different truncation ratios, while the other parameters are set as follows: $\lambda = 1.06$ μm, $a = 1$ cm, $D = 6$ cm, and $z = 10$ km. The beam width w_0 for each beamlet varies with the truncation ratio f. Figure 2 shows the intensity profiles under different propagation parameters. The panels in the first, second and third rows denote the cases of propagating in free-space and turbulent atmospheres with structure constants of $C_n^2 = 10^{-15}m^{2/3}$ and $C_n^2 = 10^{-14}m^{2/3}$, respectively. The panels in the first, second and third columns denote the cases of truncation ratios of 0.6, 0.8 and 1.1 respectively. Qualitative conclusions can be obtained from each row in Fig. 2: for different propagation environments, for the increase of truncation ratio, sidelobes that contains substantial laser energy will gradually get weakened, and more energy will be included in the central lobe. Of course, this is based on the cost of energy loss in the truncation manipulation in the source plane. It is also shown by comparing the subfigures in each column in Fig. 2 that the laser energy will spread and the power in the central lobe will decrease as the intensity of turbulence gets stronger. The one-dimensional normalized relative intensity distributions corresponding to Fig. 2 at the receiver are plotted in Fig. 3. The normalized manipulation is achieved by letting the integration of the total intensity distribution equal to 1. It is revealed that the peak intensity at the receiving plane varies with the truncation ratio. For all these three propagation circumstances with different turbulence intensities, a truncation ratio of 0.8 corresponds to a higher peak intensity at the receiving plane. In order to evaluate optimal truncation ratio under different circumstances, more quantitative conclusions should be deduced by evaluating the dependence of $J_{\rm PIB}$ on different parameters, which will be shown in the following subsections.



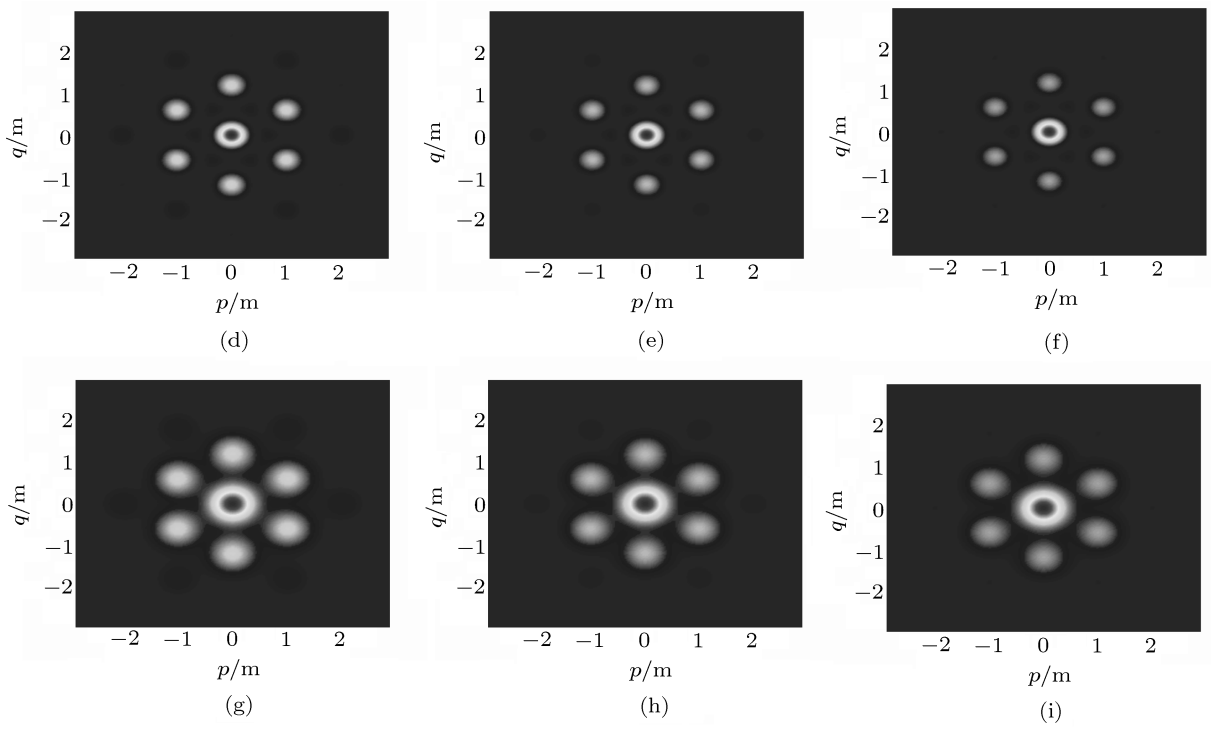


Fig. 2. Intensity profile on the receiving plane for a hexagonal-distributed 7-laser array in turbulent atmosphere with different structure constants and truncation ratios: (a) free-space, $f = 0.6$; (b) free-space, $f = 0.8$; (c) free-space, $f = 1.1$ (d) $C_n^2 = 10^{-15}m^{2/3}$, $f = 0.6$; (e) $C_n^2 = 10^{-15}m^{2/3}$, $f = 0.8$; (f) $C_n^2 = 10^{-15}m^{2/3}$, $f = 1.1$; (g) $C_n^2 = 10^{-14}m^{2/3}$, $f = 0.6$; (h) $C_n^2 = 10^{-14}m^{2/3}$, $f = 0.8$; (i) $C_n^2 = 10^{-14}m^{2/3}$, $f = 1.1$.

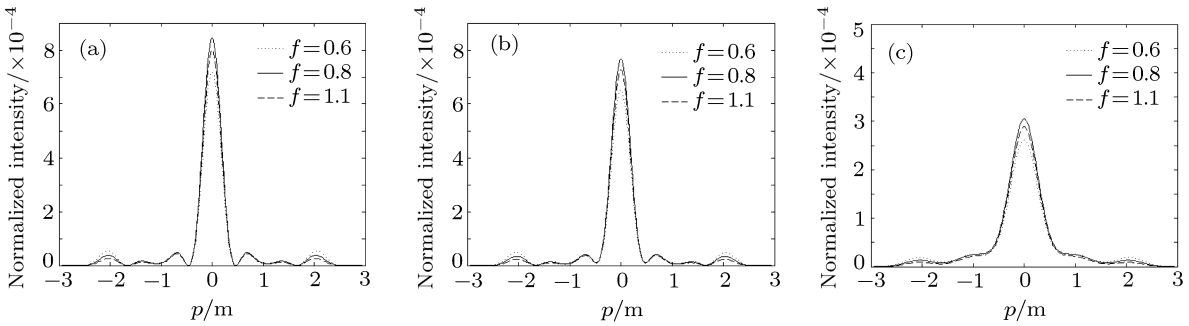


Fig. 3. One-dimensional relative average intensity profile on the receiving plane for a hexagonal-distributed 7-laser array in turbulent atmosphere with different structure constants and truncation ratios: (a) free-space; (b) $C_n^2 = 10^{-15}m^{2/3}$; (c) $C_n^2 = 10^{-14}m^{2/3}$.

3.1. Influence of laser numbers

The dependence of J_{PIB} for the 7-laser and 19-laser arrays shown in Fig. 1 on different truncation ratios is calculated by using Eq. (8) and plotted in Fig. 4. The parameters used in calculations are as follows: $\lambda = 1.06$ μm, $a = 1$ cm, $C_n^2 = 10^{-15}m^{2/3}$. For the 7- and 19-laser arrays, the optimal truncation ratios are 0.79 and 0.82 respectively when the propagation distance is $z = 10$ km. The optimal truncation ratio changes to 0.77 and 0.81 when the propagation distance is $z = 2$ km while the other parameters are kept unchanged. It can be concluded that in general, when propagating in turbulent atmosphere, the optimal truncation ratio is larger for laser array that contains more lasers, which is consistent with the conclusion deduced for propagation in free-space as shown in Fig. 6 in Ref. [14].

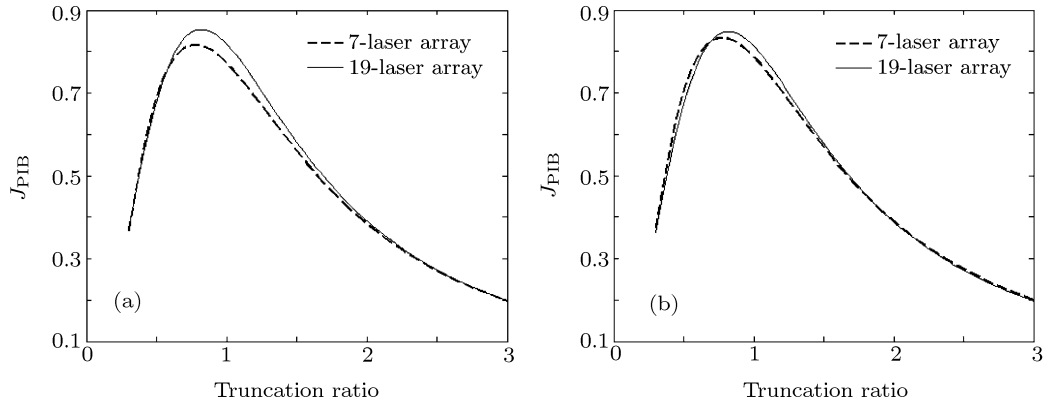


Fig. 4. Dependence of $J_{\rm PIB}$ on truncation ratio for different laser arrays (a) $z = 10$ km, (b) $z = 2$ km.

3.2. Influence of propagation distance

Propagation distance is an important parameter for practical application, like free-space communication and energy delivering fields. The optimal parameters of the whole system may vary with the propagation distance. The dependence of $J_{\rm PIB}$ on different laser arrays for different propagation distances is shown in Fig. 5. Calculation parameters are set to $C_n^2 = 10^{-15} m^{2/3}$. The optimal truncation ratios for the 7-laser array are 0.74, 0.76, 0.77, and 0.79, which are deduced from the four curves shown in Fig. 5(a) when the propagation distances are 100 m, 500 m, 2 km and 5 km respectively. The optimal truncation ratios for the 19-laser array are 0.56, 0.79, 0.81 and 0.82, respectively for the four different propagation distances as the above. It can be concluded that in general, the optimal truncation ratio shifts to a larger value as the propagation distance increases.

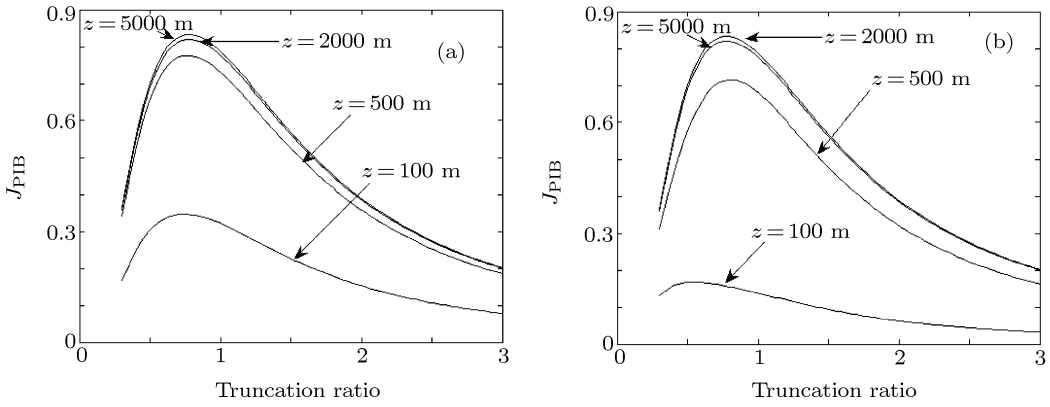


Fig. 5. Dependence of $J_{\rm PIB}$ on truncation ratio for different propagation distances: (a) 7-laser array, (b) 19-laser array.

3.3. Influence of turbulence intensity

The influence of turbulence intensity can be investigated by studying the dependence of $J_{\rm PIB}$ on truncation ratio for different structure constants, as plotted in Fig. 6. The calculation parameters are set to $\lambda = 1.06$ μm, $a = 1$ cm, $z = 5$ km. For the case of structure constants $C_n^2 = 10^{-15}$, 5×10^{-15}, 10^{-14}, 5×10^{-14}, and $10^{-13} m^{2/3}$, the optimal truncation ratios obtained are 0.79, 0.79, 0.78, 0.76, and 0.74 respectively. We can conclude from Fig. 6 that the optimal truncation ratio will shift to smaller value when the intensity of atmosphere turbulence gets stronger.

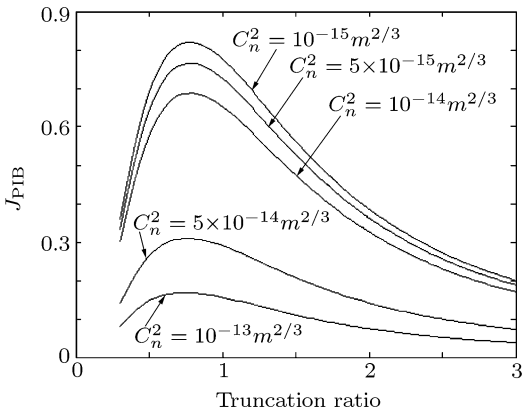


Fig. 6. Dependence of $J_{\rm PIB}$ on truncation ratio in different turbulences for the 7-laser array.

3.4. Influence of laser wavelength

Laser beams with different wavelengths may be selected for different application fields, for example, laser wavelength of about 1 μm, which requires additional eye protection, is rather proper for energy delivering use due to its relatively low atmosphere absorption. Thulium-doped fibres operating around the eye-safe wavelength of 2 μm have also been under intensive research recently.[27] In the present paper, we take three laser wavelengths, i.e., 1.06, 1.55, and 2 μm as example. The dependence of $J_{\rm PIB}$ on truncation ratio for different laser wavelengths is calculated and plotted in Fig.7. The calculation parameters are set to $a = 1$ cm, $C_n^2 = 10^{-15}m^{2/3}$, and $z = 5$ km. Calculated results show that the optimal truncation ratio for the 7-laser array is kept at the same value of 0.79 for the three different wavelengths, while for the 19-laser array the optimal truncation ratio is 0.82. It can be concluded that the optimal truncation ratio is independent of the laser wavelength.

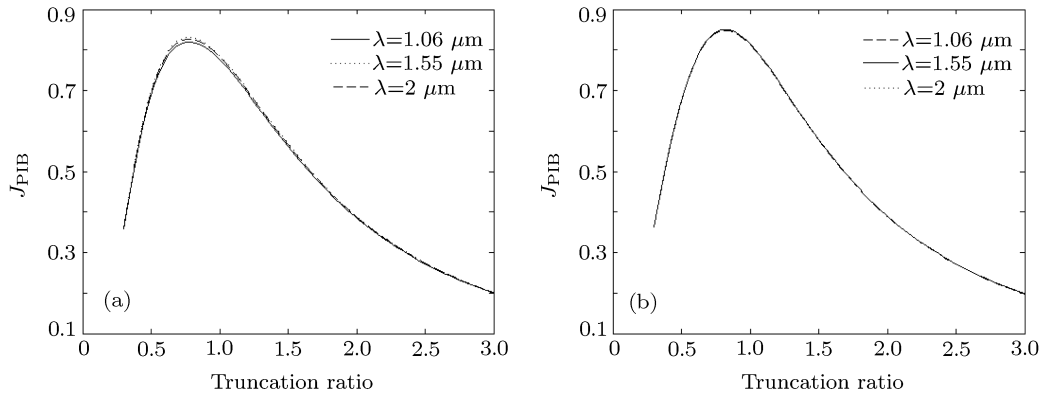


Fig. 7. Dependence of $J_{\rm PIB}$ on truncation ratio for different laser wavelengths in (a) 7-laser array, (b) 19-laser array.

4. Conclusions

Truncation manipulation is a simple but effective way to improve the intensity distribution properties of a phase-locked Gaussian beam array in the receiving plane. In this paper, we present the analytical expression for the propagation of the phase-locked truncated Gaussian beam array in turbulent atmosphere based on the extended Huygens–Fresnel principle. Power in the diffraction-limited bucket is introduced as the beam quality factor to evaluate the influence of different truncation parameters. The dependence of the optimal truncation ratio on the number of beamlets, the intensity of turbulence, propagation distance and laser wavelength is calculated and discussed. It is revealed from numerical calculation that the optimal truncation ratio is larger for the laser array that contains more lasers, and the optimal truncation ratio will shift to a larger value as the propagation distance increases and the intensity of atmosphere turbulence decreases. It is also found that the optimal truncation ratio is independent of laser wavelength. The intensity distribution expressed by Eq. (7) and conclusions deduced in this paper may offer useful reference for designing and experimenting in phase-locked beam array systems.

References

[1] Fan T Y 2005 *IEEE J. Sel. Top. Quantum Electron.* **11** 567

[2] Goodno G D, Komine H, McNaught S J, Weiss S B, Redmond S, Long W, Simpson R, Cheung E C, Howland D, Epp P, Weber M, McClellan M, Sollee J and Injeyan H 2006 *Opt. Lett.* **31** 1247

[3] Anderegg J, Brosnan S, Cheung E, Epp P, Hammons D, Komine H, Weber M and Wickham M 2006 *Proc. SPIE.* **6102** 61020U-1

[4] Augst S J, Ranka J K, Fan T Y and Sanchez A 2007 *J. Opt. Soc. Am.* B **24** 1707

[5] Goodno G D, Asman C P, Anderegg J, Brosnan S, Cheung E, Hammons D, Injeyan H, Komine H, Long W, McClellan M, McNaught S J, Redmond S, Simpson R, Sollee J, Weber M, Weiss S and Wickham M 2007 *IEEE J. Sel. Top. Quantum Electron.* **13** 460

[6] Cheung E C, Ho J G, Goodno G D, Rice R R, Rothenberg J, Thielen P, Weber M and Wickham M *Opt. Lett.* 2008

33 354
[7] Xiao R, Hou J, Liu M and Jiang Z F 2008 *Opt. Express* **16** 2015
[8] He B, Lou Q H, Zhou J, Dong J X, Wei Y R, Xue D, Qi Y F, Su Z P, Li L B and Zhang F P 2006 *Opt. Express* **14** 2721
[9] Cai Y J, Chen Y, Eyyuboglu H T and Baykal Y 2007 *Appl. Phys.* B **88** 467
[10] Eyyuboglu H T, Baykal Y and Cai Y J 2008 *Appl. Phys.* B **91** 265
[11] Ji X L and Li X Q 2008 *Acta Phys. Sin.* **57** 7674 (in Chinese)
[12] Ji X L, Zhang E T and Lü B D 2007 *J. Opt. Soc. Am.* B **25** 825
[13] Chu X X, Liu Z J and Wu Y 2008 *J. Opt. Soc. Am.* A **25** 74
[14] Zhang E T, Ji X L and Lü B D 2007 *Chin. Phys.* **16** 571
[15] Lü B D and Ma H 2000 *Appl. Opt.* **39** 1279
[16] Brosnan S J, Wichham M G and Komine H US patent 72283702
[17] Khajavikhan M and Leger J R 2008 *Conference on Lasers and Electro-Optics* (CA, USA May 2008) p CWB1
[18] Christensen S and Koski O 2007 *Conference on Lasers and Electro-Optics* (Baltimore, USA May 2007) p WC1
[19] Vorontsov M A and Lachinova S L 2008 *J. Opt. Soc. Am.* A **25** 1949
[20] Zhou P, Wang X L, Ma Y X, Ma H T, Xu X and Liu Z J 2009 *Chin. Phys. Lett.* **26** 044206
[21] Zhang Y J 2005 *Opt. Commun.* **248** 317
[22] Wen J J and Breazeale M A 1988 *J. Acoust. Soc. Am.* **83** 1752
[23] Eyyuboglu H T and Baykal Y 2004 *Opt. Express* **12** 4659
[24] Wang S C H and Plonus M A 1979 *J. Opt. Soc. Am.* **69** 1297
[25] Gradshteyn I S and Ryzhik I M 1980 *Tables of Integrals, Series and Products* (New York: Academic Press)
[26] Stickley C M http://www.darpa.mil/mto/programs/adhels/index.htm
[27] Goodno G D, Book L D and Rothenberg J E 2009 *Proc. SPIE.* **7195** 71950Y-1